

UNIVERSIDADE FEDERAL DO RIO GRANDE DO SUL
INSTITUTO DE INFORMÁTICA
CURSO DE ENGENHARIA DE COMPUTAÇÃO

LEONARDO BARLETTE DE MORAES

**Evaluation of Variability using Schmitt
Trigger on Full Adders Layout**

Work presented in partial fulfillment
of the requirements for the degree of
Bachelor in Computer Engineering

Advisor: Prof. Dr. Ricardo Reis
Coadvisor: Prof. Dr Alexandra Lackmann
Zimpeck 

Porto Alegre
July 2018

UNIVERSIDADE FEDERAL DO RIO GRANDE DO SUL

Reitor: Prof. Rui Vicente Oppermann

Vice-Reitora: Prof^a. Jane Fraga Tutikian

Pró-Reitor de Graduação: Prof. Wladimir Pinheiro do Nascimento

Diretora do Instituto de Informática: Prof^a. Carla Maria Dal Sasso Freitas

Coordenador do Curso de Engenharia de Computação: Prof. Renato Ventura Henriques

Bibliotecária-chefe do Instituto de Informática: Beatriz Regina Bastos Haro

*"If I have seen farther than others,
it is because I stood on the shoulders of giants."*

— SIR ISAAC NEWTON

AGRADECIMENTOS

Agradeço ao L^AT_EX por não ter vírus de macro...

ABSTRACT

The aggressive technology and voltage scaling which modern digital circuits are facing introduce a higher influence in metrics, as performance and power consumption, due to process variability. To mitigate that, novel techniques are proposed and tested in the literature. This work analyzes the impact on variability robustness using a technique based on the replacement of full adders internal inverters by Schmitt Triggers. Some works point that the given technique helps to improve the variability robustness at the electrical level. Therefore, analysis has been performed at layout level using the 7nm FinFET technology node from ASAP7 library and the technique was applied on four full adder designs. Performance, energy and area are taken into account. Results show up to 64.74% and 66.6% improvement in average delay and energy variability robustness, respectively.

Keywords: Formatação eletrônica de documentos. L^AT_EX. ABNT. UFRGS.

LIST OF ABBREVIATIONS AND ACRONYMS

FA	Full Adder
PVT	Process, Voltage and Temperature
CMOS	Complementary-Metal-Oxide-Semiconductor
ST	Schmitt Trigger
FinFET	Fin Field Effect Transistor
SOI	Silicon On Insulator
SCE	Short-Channel Effect
RDP	Random Dopant Fluctuation
NBTI	Negative Bias Temperature Instability
PBTI	Positive Bias Temperature Instability
WF	Work Function
WFF	Work Function Fluctuation
LG	Gate Length
HFIN	Fin Height
TSI	Fin Thickness
VTH	Threshold Voltage
ION	On-Current
IOFF	Off-Current
PDP	Power-Delay-Product
CPL	Complementary Pass-transistor Logic
TGA	Transmission Gate Adder
TFA	Transmission Function Adder
EDP	Energy-Delay-Product
CNFET	Carbon Nanotube Field Effect Transistor

FDSOI Fully Depleted Silicon On Insulator
OTS Optimized Transistor Sizing
SRAM Static Random-Access Memory
PMOS P-channel Metal-Oxide-Semiconductor
NMOS N-channel Metal-Oxide-Semiconductor
EDA Electronic Design Automation
PDK Process Design Kit

 ASAP Arizona State Predictive PDK
M2 Metal 2
MC Monte Carlo
PTM Predictive Technology Model
NT Near-Threshold

LIST OF FIGURES

Figure 1.1 Comparison between Bulk CMOS (left) and FinFET (right) transistors.	13
Figure 2.1 Transistor Variability	15
Figure 2.2 Metal gate fabrication ideal and real aspects.....	16
Figure 2.3 a) General ST hysteresis curve b) Classical CMOS ST Topology c) Typical signal filtering with ST.....	19
Figure 3.1 Full Adders with internal inverters to be replaced highlighted.	22
Figure 3.2 Original and modified STs side-by-side	23
Figure 3.3 Technology layers and original Mirror CMOS Layout	24
Figure 3.4 Test Bench.	26
Figure 4.1 Robustness improvements for each Full Adder at nominal operation.....	29
Figure 4.2 Robustness improvements for each Full Adder at near-threshold operation.	31
Figure 4.3 Energy measures for the Sum output at Nominal operation.....	31
Figure 4.4 Energy measures for the Carry Out output at Nominal operation.....	31
Figure 4.5 Energy measures for the Sum output at Near-Threshold operation.....	31
Figure 4.6 Energy measures for the Carry Out output at Near-Threshold operation.....	31
Figure 4.7 Original Mirror CMOS (a) and Mirror CMOS with ST technique (b) layouts.....	33
Figure 4.8 Original TGA (a) and TGA with ST technique (b) layouts.....	34
Figure 4.9 Original TFA (a) and TFA with ST technique (b) layouts.....	35
Figure 4.10 Original HYBRID (a) and HYBRID with ST technique (b) layouts.	36

LIST OF TABLES

Table 1.1 Truth Table of Full Adders	12
Table 2.1 Design impact on performance and power due to different types of variability	15
Table 3.1 Key layer lithography assumptions, widths and pitches	24
Table 3.2 Parameters applied in the electrical simulations	25
Table 4.1 Delay measures for nominal voltage operation.....	28
Table 4.2 Energy measures for nominal voltage operation.....	28
Table 4.3 Delay measures for near-threshold operation.....	30
Table 4.4 Energy measures for near-threshold operation.....	30
Table 4.5 Full Adders areas and respective technique area impact.....	32

CONTENTS

1 INTRODUCTION.....	11
2 VARIABILITY EFFECTS AND MITIGATION TECHNIQUES	14
3 METHODOLOGY	21
3.1 Layout Design.....	23
3.2 Electrical Simulation	25
4 RESULTS AND DISCUSSION.....	27
4.1 Nominal Operation	27
4.2 Near-Threshold Operation.....	28
4.3 Penalties	30
5 CONCLUSIONS	37
REFERENCES.....	38

1 INTRODUCTION

The technology scaling over the years have significantly increased the density of transistors present on chips. Alongside, with the advance over transistor technology, new challenges were introduced due to the scale down, as aging effects, high power consumption due to leakage current and an increase in the sensibility to transient faults due to radiation and process variability (ABBAS et al., 2015).

The same technology scaling that allowed the increase in transistor density also allowed a voltage scaling due to the shortening of gate dimensions, internal capacitances and resistances. These two combined events contributed to the emergence, growth and current dominance of mobile applications over its counterpart. This new context, introduced a concern for battery lifespan which these applications are dependent (ISLAM et al., 2010).

The ascending number of mobile applications that depends on highly sophisticated processing schemes with a limited power-supply capability of today's batteries brings conflicting needs. The need to explore high-performance designs and implementations to meet the speed constraints for real-time applications and, simultaneously, consider low-power design approaches to extend the battery life of portable devices (SHOARINEJAD; UNG; BADAWY, 2003).

Due to the new power consumption concern, novel types of logic blocks for chips started being designed for low power. One of the most present logic blocks in computer systems is the Full Adder (FA). It plays a central role in performing general arithmetic operations such as addition, subtraction, division, shift and so on. The full adder operation adds two bits considering the Carry Out value from a less significant stage. It follows the equations 1.1 and 1.2 with the Truth Table 1.1.

$$\text{Sum} = (A \oplus B) \oplus Cin \quad (1.1)$$

$$\text{Cout} = (A \wedge B) \vee Cin \wedge (A \oplus B) \quad (1.2)$$

Adder cells define the throughput and are employed in the processor's executive, floating-point, and memory address generation units. Due to its absolute numbers in microprocessors and their part on the critical path of electronic systems, any improvements over adding blocks generates a considerable improvement in the whole system

Table 1.1: Truth Table of Full Adders

Input			Output	
A	B	Cin	Sum	Cout
0	0	0	0	0
0	0	1	1	0
0	1	0	1	0
0	1	1	0	1
1	0	0	1	0
1	0	1	0	1
1	1	0	0	1
1	1	1	1	1

because of the huge influence of power, timing and area characteristics on the system design (SHOARINEJAD; UNG; BADAWY, 2003).

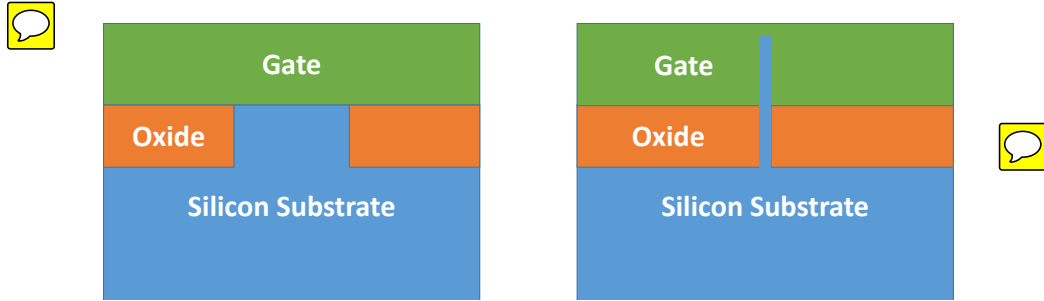
Moore's law predicts that the number of transistors per square on integrated circuits will double every year and it has been guiding the industry trending for decades. However, continue with scaling in the bulk Complementary metal-oxide-semiconductor (CMOS) technology has been no straightforward task. At deep nanotechnology nodes, each chip may show different behavior due to process variations during the manufacturing steps. Variations that influence the circuits metrics such as performance and power consumption, hastening the circuit degradation and making it deviate from its correct operation (ABBAS et al., 2015) (NASSIF, 2008).

In this context, this work employs a technique using Schmitt Trigger (ST) inverters for process variability mitigation on different Full Adder topologies with priority on power consumption variations. Performance, power, and area penalty were analyzed alongside variability robustness. 

Promising new commercial technologies based on the Fin Field Effect Transistor (FinFET) devices have been introduced to maintain the technology scaling. The process variability impact on those technologies have shown to be less present, although it can not be ignored, being necessary more research concerning the characterization of process variability effect on emerging technologies.  

FinFET technology is built on a Silicon on Insulator (SOI) substrate with a conducting channel that rises above the level of the insulator, creating a thin silicon structure, the gate as shown in Figure 1.1. The channel being surrounded from three dimensions by the gate results in a superior control, reduced short-channel effect (SCE) and eliminated random dopant fluctuation (RDF) effect due to the fully depleted channel that causes less sensitivity to process variations (TAUR; NING, 2013).

Figure 1.1: Comparison between Bulk CMOS (left) and FinFET (right) transistors.



This work is divided into five further sections: Variability Effects and Mitigation Techniques, with a theoretical foundation about variability. Motivation and Objectives, explaining in more details this work's objective. Methodology, presenting how results were achieved with its experimental setup. The Results and Discussion presenting the simulation results and its analysis. And, lastly, the Conclusions.

2 VARIABILITY EFFECTS AND MITIGATION TECHNIQUES

Standard CMOS devices have been optimized for high-speed and low-power consumption through its lifetime being the backbone of almost all modern digital circuits. The periodic process of technology scaling has resulted in faster and more energy efficient transistor than the previous generation. As channel lengths shrank below 50nm, the ratio of device size to atom-size becomes smaller, hence, a variable structure at the atomic scale has an increased effect on device behavior. There have been advances to reduce the loss of precision due to the manufacturing process. However, the intrinsic quantum-mechanical limitations cannot be overcome, with their impact increasing as the technology shrinks further.



Variability can occur in both spatial and temporal domains with deterministic and stochastic fluctuations (WALKER et al., 2010). In summary, variability consists of deviation of characteristics, internal or external, to the circuit, which can determine its operational features such as power and delay. These characteristics, or factors, as we addressed them for the rest of this work, can be divided into three types:

Environmental Factors: Caused by temperature fluctuations and voltage drops. Voltage drops occurs due to abrupt changes in the switching activity, causing large current transients in the system, which can occur locally as well globally across the die (NASSIF, 2008).

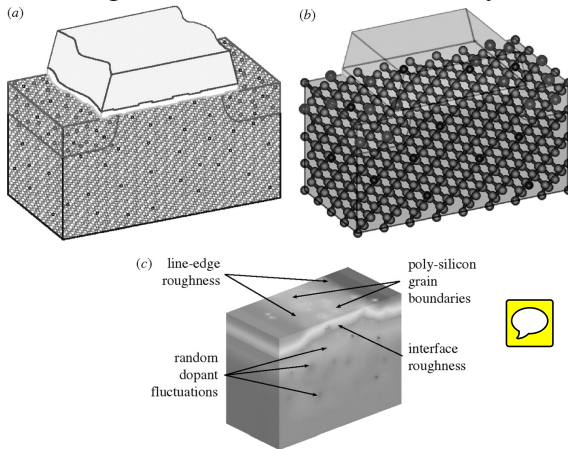
Reliability Factors: Related to the aging process of the circuit, it is introduced by negative bias temperature instability (NBTI), positive bias temperature instability (PBTI), electromigration, time dependent dielectric breakdown, gate oxide integrity, thermal cycling and hot carrier injection (NASSIF, 2008).

 **Physical Factors:** It is related to variations caused by the manufacturing process, which results in deviations in the electrical parameters defining the behavior of active and passive devices. Those variations can be divided in three types of mechanisms: Systematic, they repeat over many chips or wafers. Design dependent, being particular to each circuit design. And Random, which depends on the random aspects of process manufacturing, as shown in Figure 2.1 (NASSIF, 2008).

Additionally, the technology scaling and manufacturing tolerances are not correspondingly moving side by side. For instance, the pace at which the effective channel length is reduced is faster than the improvement of mask fabrication error and mask overlay control (NASSIF, 2008) (AGHABABA; AFZALI-KUSHA; FOROUZANDEH,

2009).

Figure 2.1: Transistor Variability



Source: (WALKER et al., 2010)

These three types of variabilities, in conjunction, may prevent circuits from meeting their performance and power goals. Table 2.1 demonstrates the design impact of performance and power due to different types of variability.

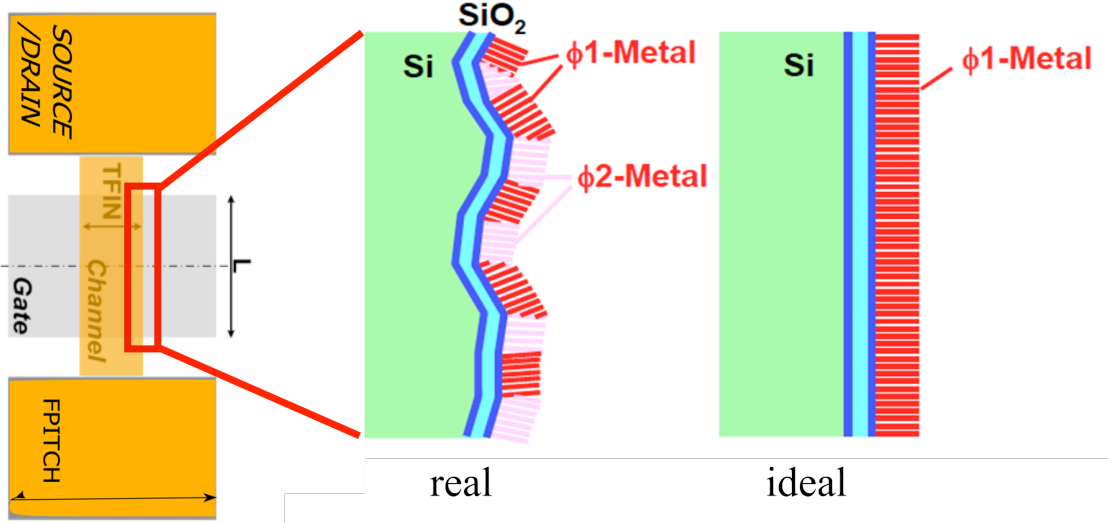
Table 2.1: Design impact on performance and power due to different types of variability
Source: (RAHIMI; BENINI; GUPTA, 2016)

Property	Ease of measuring	Variability	Effects of Variability	Effect of missing specification
Performance	Medium	Medium: up to 60%	L, W, R, C, V _{th} , μ	Slower product, yield, timing error
Leakage Power	Easy	Large: up to 148%	L, V _{th} , μ , tox	Shorter battery life, yield, heat
Dynamic Power	Difficult	Workload dependent	C, α	Shorter battery life, heat

This work evaluates the effects caused by the physical variability. In FinFET, the physical variations are responsible for deviations in the device work function (WF), gate length (LG), fin height (HFIN), fin thickness (TSI) and parasitic resistances. It is shown in (MEINHARDT; ZIMPECK; REIS, 2014) that work function fluctuation (WFF) is the main cause of threshold voltage (VTH) variations. Alongside, in (WANG et al., 2011) is shown the high correlation between the variability in the on (I_{ON}) and off (I_{OFF}) currents and V_{TH} fluctuation in the presence of granularity of the metal gate. The main cause of WFF is due to its dependency over the orientation of its metal grains. In the real fabrication process, metal gate devices are generally produced using multiple types of metal with different work functions randomly aligned as depicted in Figure 2.2. In the ideal fabrication process, metal gate devices have the gates manufactured with uniformly aligned metal and then, they have very low WFF deviation (ZIMPECK et al., 2016)

At circuit level there is multiple techniques to predict and prevent errors: Tuning CMOS knobs, circuit topology optimizations, self-timed circuits, temporal and logical error masking, relaxed retiming and graceful degradation, and inexact circuits. Although,

Figure 2.2: Metal gate fabrication ideal and real aspects.



Source: (MEINHARDT; ZIMPECK; REIS, 2014)

there are few approaches to decrease the process variability at its core. It is due to the technology dependency present in this problem (RAHIMI; BENINI; GUPTA, 2016).

It can be observed that many works try to indicate the most robust design for a given type of circuit. For example, in (DOKANIA; IMRAN; ISLAM, 2013) twelve different Full Adder topologies are analyzed considering delay, power and Power-Delay-Product (PDP) variability. It is used a 16nm bulk CMOS technology node in SPICE simulations with Process, Voltage and Temperature (PVT) variability being considered and Monte Carlo simulations performed. The authors concluded that Cell A, CLRCL and Cell B full adders presented the best results for all three metrics (Delay, Power and PDP).

In (AMES et al., 2016) the effects of PVT variability in different full adder designs are investigated. The simulations are performed in HSPICE with the bulk CMOS 32nm node technology. With Transmission Gate Full Adder (TGA) and Transmission Function Adder (TFA) architectures showing acceptable behavior under PVT variability with the lowest power consumption sensibility amongst the tested full adders - 11x smaller in comparison with Complementary Pass Transistor Logic (CPL) Full Adder.

In (ISLAM; HASAN, 2011) various popular 1-bit digital summing circuits functionality and robustness are analyzed in light of PVT variations with the best full adder being simulated in Carbon Nanotube Field Effect Transistor (CNFET) technology for comparison with the bulk CMOS version. The simulations are carried at the 22nm bulk CMOS and CNFET technology node in HSPICE. Its results show that the TGA has the strongest PVT variability robustness and its CNFET version provides over 3x, 1.14x and

1.1x less propagation delay, power dissipation and energy delay product (EDP) variations, respectively. This work does not consider the total power consumption of each full adder separately.

Some articles analyze the adoption of new technologies: (GUDURI; ISLAM, 2015) proposes a hybrid of bulk CMOS and CNFET Full Adder at 16nm in deep sub-threshold operation region for ultralow-power applications simulated in SPICE which showed some improvement over its bulk CMOS Full Adder counterpart achieving 5% and 1% improvement in power, power-delay and energy-delay products and their variability, respectively.

In (ISLAM; AKRAM; HASAN, 2011) a new subthreshold-FinFET Full Adder is proposed and compared over multiple full adders showing huge metric improvements provided by the FinFET technology up to 2.22x improvement in power variability. It was simulated in 32nm predictive technology model on HSPICE.

It is notable that none of these works consider a layout approach for its simulations and do not address any novel general technique which can be applied to a range of different types of circuits. Although, some works introduce novel designs.

(FEDERSPIEL et al., 2012) presents reliability comparison between 28nm bulk CMOS and Fully Depleted Silicon On Insulator (FDSOI) technologies at layout level, with FDSOI showing 32% improved performance, 40% reduced power consumption and improved matching, with its intrinsic reliability behavior similar to 28nm bulk at the device level. (ALIOTO; PALUMBO, 2007) presents a study about the delay variability caused by supply variations in the TGA. The experiments were performed at 90nm and 180nm bulk CMOS Technology in Spectre at layout level. It showed that lower supply voltages bring more delay variability to the circuit with the TGA presenting worse results 15% (25%) for the 90 nm (180 nm) in comparison to static logic.

Some works focus on evaluating techniques: In (ZIMPECK et al., 2016) three dimensioning methods are applied on multiple circuits and their impact on variability robustness is analyzed. The simulations were performed considering a 14nm FinFET technology using HSPICE tool. The authors concluded that the Optimized Transistor Sizing (OTS) technique has the best ratio between nominal PDP and PDP under process variability.

(AHMADI; ALIZADEH; FOROUZANDEH, 2017) introduces a new technique to improve the performance of digital circuits in the presence of variations. It consists of a hybrid of two former methods to prevent errors due to delay variations. The simula-

tions were performed with a 45nm predictive technology using HSPICE and applied on ITC'99 and ISCAS'89 benchmarks circuits. The results show that this hybrid technique can tolerate process variations up to 27.3% better than state-of-the-art techniques.

Among these works there is (DOKANIA; ISLAM, 2015) on which a novel technique based on the replacement of Full Adder's internal inverters with low voltage Schmitt Triggers for PVT variability robustness improvement is originally introduced and applied on seven different full adder designs. The simulations were performed using the 16nm bulk CMOS predictive technology model in SPICE. It presented significant variability improvement up to 4.8x in PDP. Although, the improvements occur at the cost of an increase in the area and power dissipation of each design. 

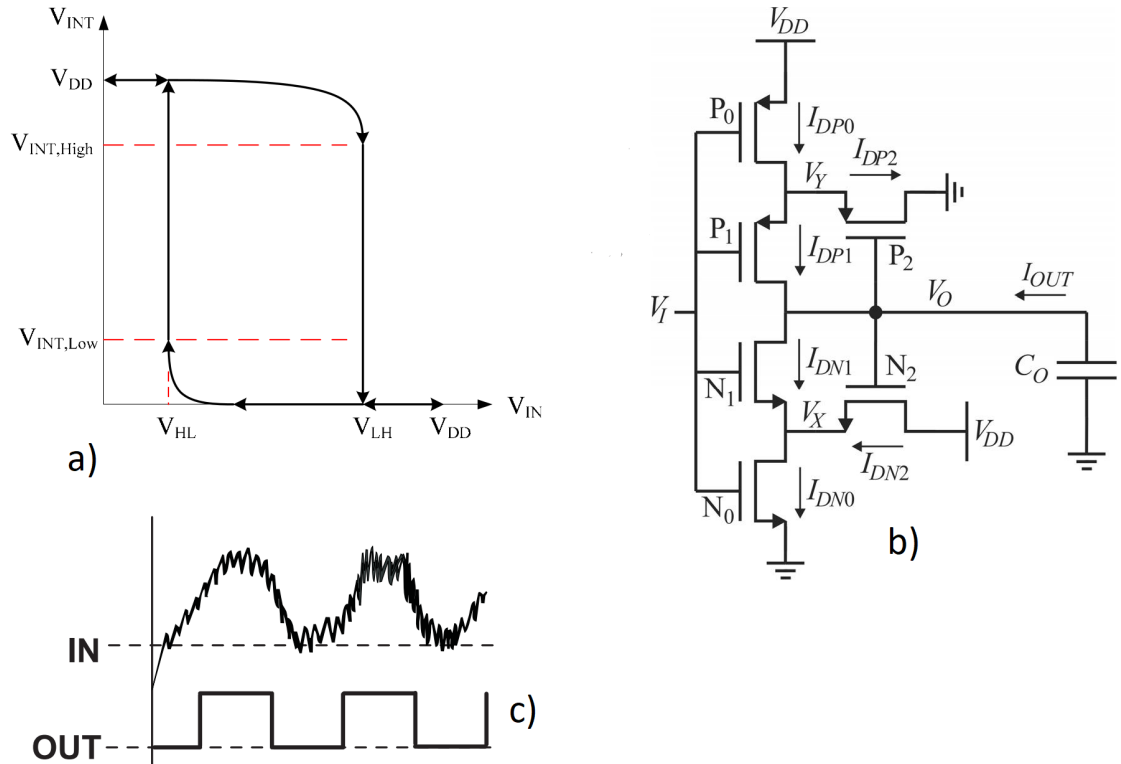
Schmitt triggers are commonly used as internal circuits on systems to provide enhanced noise tolerance and robustness against random variations in the input waveforms. On a typical input (non-Schmitt trigger), its binary value will switch at the same point on the rising and falling edges. With a slow rising edge, the input will change near the threshold point. When the switching occurs, it will require current from the supply source. With current being pushed from the supply, it can cause a voltage drop across the circuit causing a shift in the threshold voltage.

If the threshold shifts, it will cross the input causing it to switch again. It can go indefinitely causing oscillation. The same thing can happen if there is noise on the input. Schmitt Triggers are applied in these cases to filter noise introducing superior and inferior threshold voltages, as shown in Figure 2.3.c. The difference between the thresholds is called Hysteresis (COCKRILL, 2011), its curve is shown at 2.3.a. According to the Schmitt Trigger behavior, it can mitigate the influence of variations in the inputs product of PVT variability. In figure 2.3.c is shown a classical CMOS Schmitt Trigger design.

This technique is tested in several works: In (AHMAD et al., 2016) it is presented a novel Schmitt-trigger-based single-ended 11 Transistor Static random-access memory (SRAM) cell. It analyses its performance against seven different SRAM topologies. The novel cell showed the least energy consumption per operation with the smallest leakage power and a 6.9x higher Ion/Ioff ratio. Further PVT variability simulations confirmed the robustness of the design regarding read and write operation. The simulations were carried in 22nm predictive technology using HSPICE.

(MOGHADDAM; MOAIYERI; ESHGHI, 2017) presents a Schmitt trigger (ST) buffer using CNFET. It was evaluated against other two buffers and showed, on average,

Figure 2.3: a) General ST hysteresis curve b) Classical CMOS ST Topology c) Typical signal filtering with ST.



Source: (COCKRILL, 2011)

68% higher critical charge and 53% lower energy consumption and a huge gain considering PVT variability robustness. The simulations were carried in 16nm Stanford CNFET model using HSPICE.

Alongside, in (TOLEDO; ZIMPECK; MEINHARDT, 2016) the ST technique is applied on four Full Adders. It presented promising results regarding the power deviation due to the process variability with a decrease up to 79% with a drawback of a significant increase in average energy consumption. The simulations were performed with the 16nm technology predictive technology model in NGSPICE.

3 METHODOLOGY

For the experiments, there were considered four different types of Full Adders topologies to evaluate their robustness to process variability with their internal inverters replaced by Schmitt Triggers. The Full Adders listed below have been chosen due to their promising results in related works (AMES et al., 2016) (DOKANIA; ISLAM, 2015) (DOKANIA; IMRAN; ISLAM, 2013):

1. Complementary MOSFET Adder (CMOS)
2. Transmission Gate Adder (TGA)
3. Transmission Function Adder (TFA)
4. Hybrid Full Adder

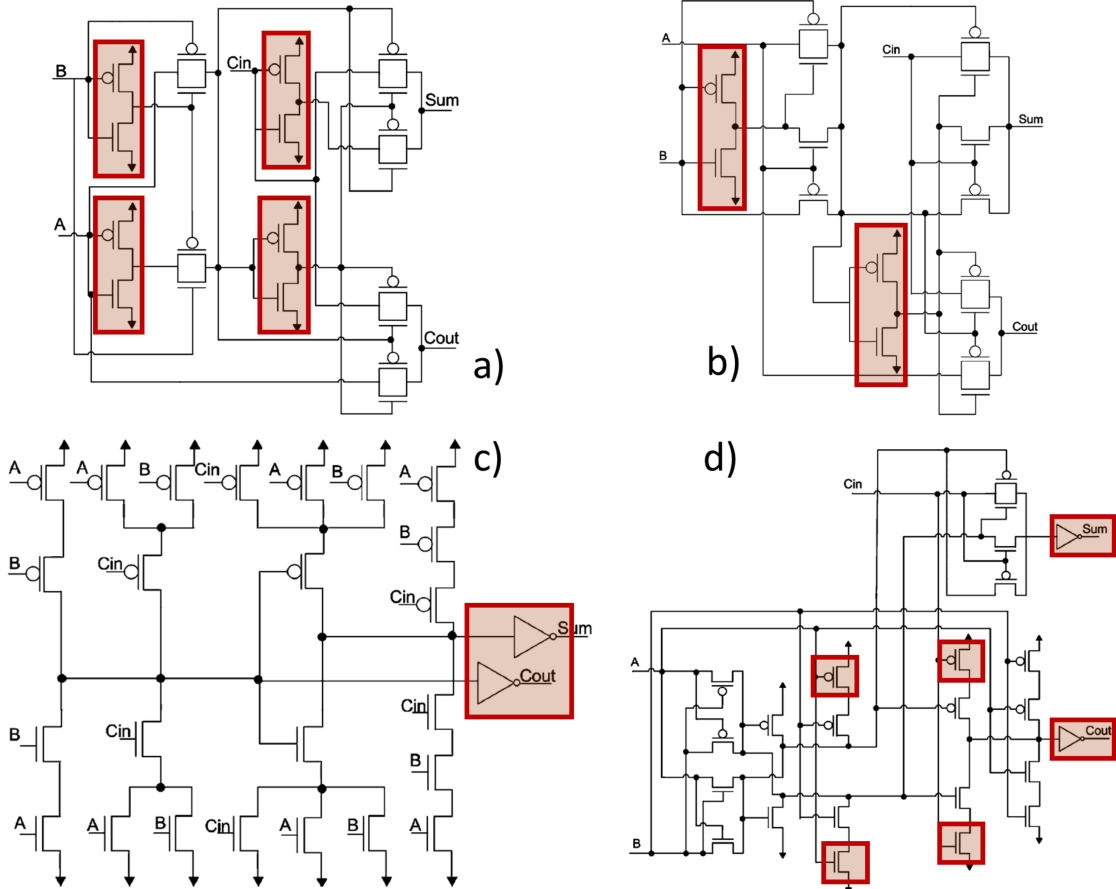
The CMOS Full Adder is considered the most traditional Full Adder topology containing 28 Transistors arranged in a pull-up and pull-down networks, which are logically complementary. It has a full voltage swing and buffered Sum and Cout signal and the advantages of good conductibility and robustness when working with novel technologies and low voltages. However, it has high capacitance because each input is connected to the gate of at least a p-channel metal-oxide-semiconductor (PMOS) and n-channel metal-oxide-semiconductor (NMOS) device additionally, it shows the impact of the pull-up network that makes the circuit slower due to the low mobility of its holes (BECKETT, 2002) (DEVADAS; KISHORE, 2017) (ISLAM; HASAN, 2011).

Transmission Gate Full Adder (WESTE; ESHRAGHIAN, 1985) contains 16 transistors, and is a high speed and low power design. However, shows low driving capability which may be unacceptable in some cases where there is a long chain of full adders due to the increase in delay (ISLAM; HASAN, 2011). The Transmission Function Adder is based on transmission gates as well, containing 20 transistors, working satisfactorily with low voltages but losing performance when cascaded due to the lack of supply/ground contacts and, consequently, driving capability (NAVI et al., 2009). Both TFA and TGA generate the XOR function ($H = A \text{ XOR } B$) followed by an inverter which produces the XNOR function (H'). H and H' are used to control the transmission gates generating the Sum and Cout outputs. The inverter generates delay between H and H' , which will cause the transmission gates to behave as pass transistors, that may introduce glitches and consequently, increase the power consumption of these cells. Additionally, TGA contains three inverters, one more than TFA. The inverters switching introduce more short-circuit

power (SHAMS; BAYOUMI, 2000).

Inspired by CMOS and CPL Full Adders architectures, the Hybrid Full Adder (NAVI et al., 2009) contains 26 transistors, with the main advantage of a high output signal and low power properties. Although, the design shows high input capacitance for specific input vectors. The Full Adder designs are shown in Figure 3.1.

Figure 3.1: Full Adders with internal inverters to be replaced highlighted.

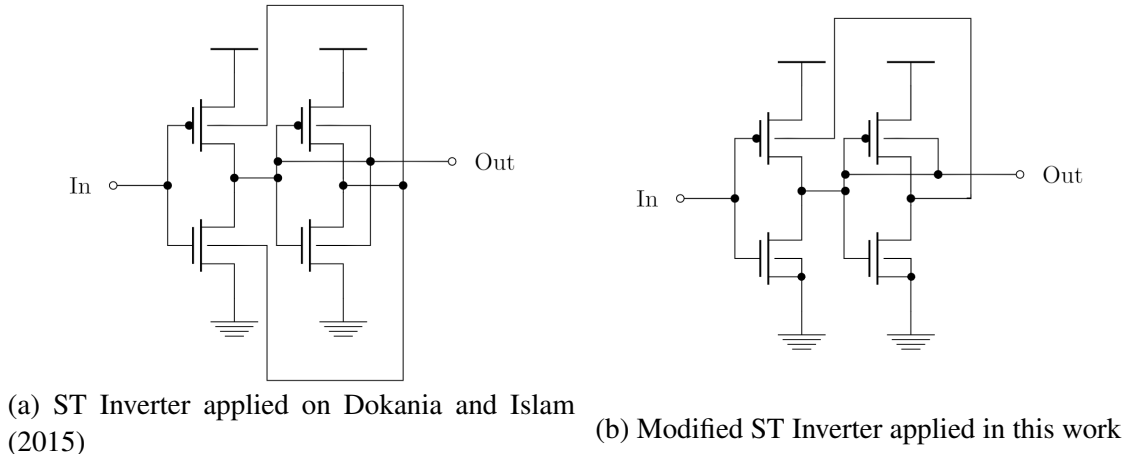


Transmission Function Adder (a), Transmission Gate Adder (b), Mirror CMOS Adder (c) and Hybrid Full Adder (d). Source: (TOLEDO; ZIMPECK; MEINHARDT, 2016)

A variety of CMOS Schmitt Trigger designs have been proposed and implemented over the years, with the conventional 6T-CMOS Schmitt Trigger proposed in (DOKI, 1984) exhibiting the wanted characteristics of different high-to-low and low-to-high transition threshold voltages, giving rise to hysteresis. The ST inverter circuit used in this work was inspired by (ZHANG; SRIVASTAVA; AJMERA, 2003) and modified in (DOKANIA; ISLAM, 2015) to achieve the desired inverting characteristic, as shown in Figure 3.2a. It is designed for operation at a supply voltage of 0.4V in order to achieve low power consumption, and consists of the junction of two inverters where the output from the second one will be the bulk for the first one.

In this design a dynamic body-bias technique is applied through a feedback mechanism to a standard CMOS inverter circuit, thus allowing a change in the threshold voltages of two MOSFETs, implying a change in the switching voltage.

Figure 3.2: Original and modified STs side-by-side



(a) ST Inverter applied on Dokania and Islam (2015) (b) Modified ST Inverter applied in this work



3.1 Layout Design

All Full Adders layouts were designed using the Virtuoso Electronic Design Automation (EDA) tool from Cadence® with the process design kit (PDK) of 7-nm FinFET or Arizona State Predictive PDK (ASAP7) from the Arizona State University in partnership with ARM (CLARK et al., 2016). This PDK was chosen due to realistic design conjecture regarding the current design competencies. Due to limitations of ASAP7 technology, it is not possible to connect the NMOS bulks separately due to the shared substrate. Given that, the Schmitt Trigger behavior is preserved with only minor changes between charging and discharging delays due to the difference between PMOS and NMOS threshold voltages. The ST applied in this work is shown at Figure 3.2b.

The main PDK rules and lithography assumptions considered in this work are shown in Table 3.1. To exemplify the PDK layers, the traditional CMOS Full Adder layout is shown in Fig. 3.3. For all layouts it was used a dense 7.5 M2 (Metal 2) track cell, baseline resulting in a 270nm cell height. This corresponds to three fins for each transistor. To make the bulk connections it is necessary a TAP-Cell. It is responsible to connect the NMOS and PMOS bulks to supply/ground, respectively, being possible to connect the PMOS bulks to another node. It is a technology restriction needed for the proper function of the circuit. Its layout has a length of 108nm resulting in an area of

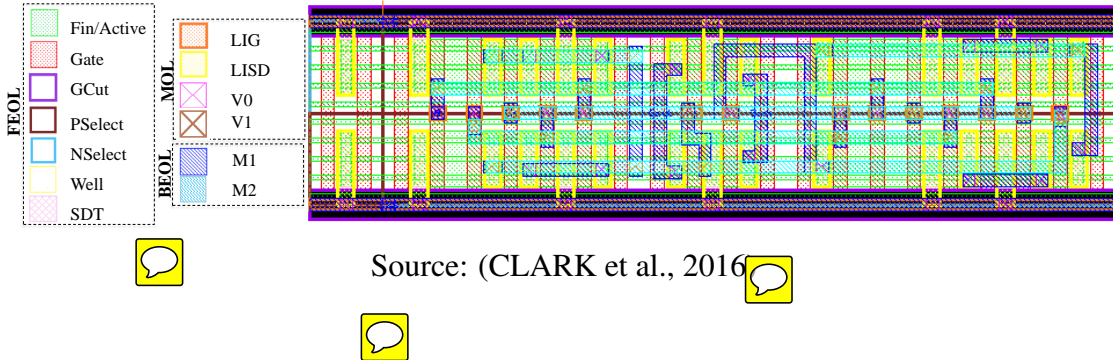


$0.02916 \mu\text{m}^2$.

Table 3.1: Key layer lithography assumptions, widths and pitches

Layer	Lithography	Width/drawn (nm)	Pitch (nm)
Fin	SAQP	6.5/7	27
Active (horizontal)	EUV	54/16	108
Gate	SADP	21/20	54
SDT/LISD	EUV	25/24	54
LIG	EUV	16/16	54
VIA0-VIA3	EUV	18/18	25
M1-M3	EUV	18/18	36

Figure 3.3: Technology layers and original Mirror CMOS Layout



Source: (CLARK et al., 2016)

3.2 Electrical Simulation

The simulations were carried out in HSPICE considering the new netlist obtained after the physical verification flow and the parasitic capacitances extraction. Each full adder was designed with and without the Schmitt Triggers replacement to consider the penalties due to the adoption of the ST technique in terms of area, energy and performance.



The process variability evaluation was taken through 2000 Monte Carlo (MC) simulations varying the threshold voltage of the PMOS and NMOS devices according to a Gaussian distribution considering a 3σ deviation and a 5% variation on nominal values. For all experiments, it was observed maximum values, mean (μ), standard deviation (σ) and normalized standard deviation (σ/μ) for each metric: delay, power and energy, where σ/μ represents the sensibility of the cell to process variability.

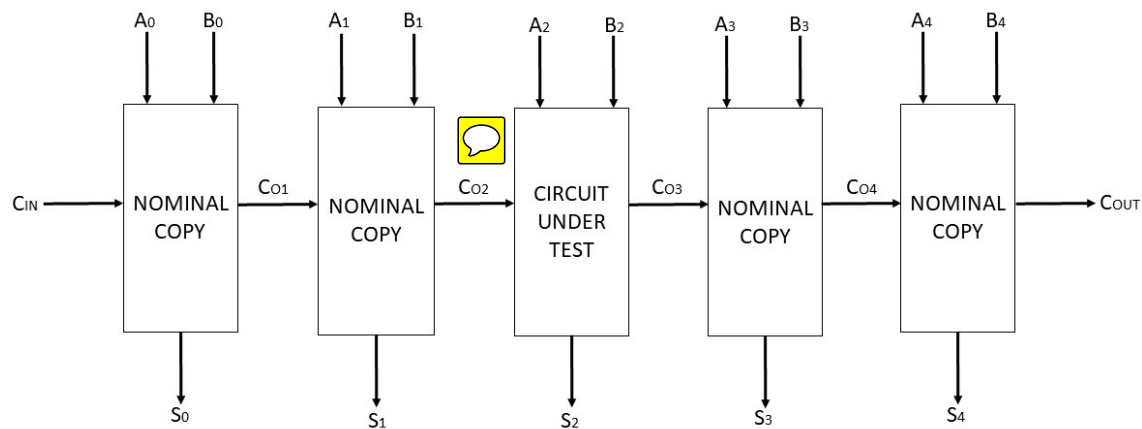
The reference values from ASAP7 technology for electrical simulations are shown in Table 3.2. To avoid underestimating effects of realistic input waveforms on design metrics, the simulations were carried under a 5-bit ripple carry adder using copies of the

1-bit full adder cell with design metrics being calculated for the middle cell as shown in Figure 3.4.

Table 3.2: Parameters applied in the electrical simulation 

Parameter	7nm	
Nominal Supply Voltage	0.7 V	
Gate Length (LG)	21nm	
Fin Width (WFIN)	6.5nm	
Fin Height (HFIN)	32nm	
Oxide Thickness (TOX)	2.1nm	
Channel Doping	$1 \times 10^{22} m^{-3}$	
Source/Drain Doping	$2 \times 10^{22} m^{-3}$	
Work Function	NFET	4.372
	PFET	4.8108

Figure 3.4: Test Bench.



Source: (DOKANIA; ISLAM, 2015)

4 RESULTS AND DISCUSSION

The results are organized into two main analysis: the set of full adders were evaluated at nominal conditions and operating at a near-threshold (Nt) region with supply voltage equal to 0.4V. In both cases, the process variability is considered and simulations with and without the ST technique is performed. To highlight the improvements and drawbacks of the ST technique for each FA, results also show the relation (Δ) between the deviation of traditional and ST circuits.

4.1 Nominal Operation

At nominal supply voltage, carry-out generation is always the critical path, considering or not the variability effects. According to the Table 4.1 and Table 4.2, it is possible to observe an increase on the mean of delay and energy for all circuits when the ST technique is inserted in the design compared to traditional one.

TFA presented the best performance and the lowest energy consumption for nominal voltage operation. However, TFA presented high maximum values and large standard deviation that are essential points to be considered. These points are a consequence of the heavy signal degradation on the TFA outputs, leaving the TFA for high-performance applications more indicated to technology nodes with low process variability sensibility. The CMOS adder showed the smallest standard deviations being the most recommended for technology nodes with high variability.

Also, these results for 7nm ASAP7 technology considering layout are in the face of the results found to 16nm Predictive Technology Model (PTM) High-Performance technology (TOLEDO; ZIMPECK; MEINHARDT, 2016). 7nm layout with ASAP7 technology shows significant improvement on the energy robustness (over 18%) at nominal voltage and in some cases also in the delay robustness to process variability.

According to Table 4.2, ST circuits increased the mean energy about close two times considering the energy necessary to cover all timing arches to the SUM output. The effect is lighter on the Carry-Out total energy. But, although this penalty, the benefits of ST technique on the cell robustness against process variability are considerable. All the ST FA circuits have the deviation reduced. Hybrid presented the best improvement on energy robustness, with 30% more stability. Fig. 4.1 resumes the improvement reached with the ST technique on Delay and Energy. Only TGA and TFA do not have total improve-

ment, with some degradation on delay for the SUM output on TGA and the Carry-out on TFA. However, the deviation is reduced to all the other cases significantly. 

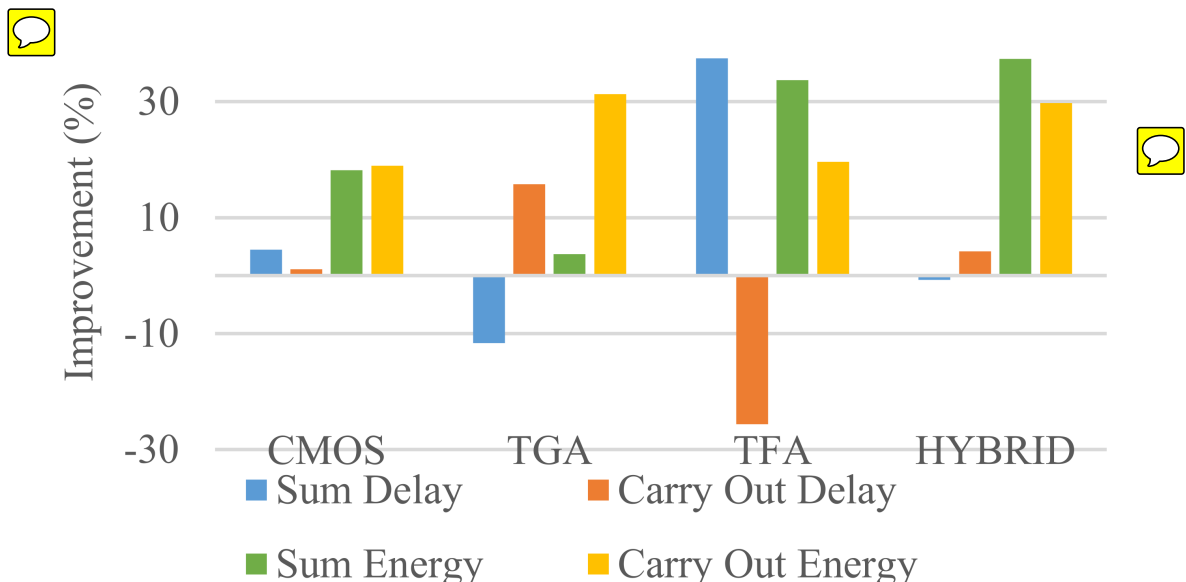
Table 4.1: Delay measures for nominal voltage operation.

@Nominal Voltage	Delay									
	SUM					CARRY OUT				
	Max (ps)	μ (ps)	σ (ps)	σ/μ (%)	Δ (%)	Max (ps)	μ (ps)	σ (ps)	σ/μ (%)	Δ (%)
CMOS	93.19	16.11	3.83	23.31	4.46	104.48	27.38	5.92	21.60	1.05
CMOS ST	117.19	21.98	4.98	22.27		120.01	33.09	7.08	21.38	
TGA	63.13	14.51	3.28	27.94	-11.65	60.11	16.32	4.28	28.54	15.77
TGA ST	77.71	17.63	3.80	31.20		71.82	21.19	4.77	24.04	
TFA	1016.90	12.63	10.62	58.94	37.43	2010.20	14.74	13.77	77.59	-25.64
TFA ST	83.52	15.39	4.16	36.88		2030.50	22.72	37.42	97.48	
HYBRID	117.57	18.15	4.42	23.72	-0.75	65.29	17.30	4.18	25.57	4.20
HYBRID ST	192.48	25.92	6.55	23.90		96.40	23.27	5.64	24.50	

Table 4.2: Energy measures for nominal voltage operation.

@Nominal Voltage	Energy									
	SUM					CARRY OUT				
	Max (fJ)	μ (fJ)	σ (fJ)	σ/μ (%)	Δ (%)	Max (fJ)	μ (fJ)	σ (fJ)	σ/μ (%)	Δ (%)
CMOS	69.07	12.89	2.97	23.00	18.21	83.43	20.88	3.52	16.87	18.91
CMOS ST	93.07	20.26	3.81	18.81		98.66	30.69	4.20	13.68	
TGA	60.36	11.78	2.36	20.04	3.71	92.71	13.54	4.15	30.61	31.32
TGA ST	90.61	22.99	4.44	19.30		93.03	24.79	5.21	21.03	
TFA	21.94	4.45	0.92	20.67	33.73	29.74	4.96	1.14	22.99	19.62
TFA ST	29.28	10.59	1.45	13.70		53.74	10.58	1.96	18.48	
HYBRID	86.45	12.99	3.63	27.97	37.38	93.88	19.99	3.89	19.48	29.74
HYBRID ST	87.13	23.67	4.15	17.52		98.85	35.58	4.87	13.69	

Figure 4.1: Robustness improvements for each Full Adder at nominal operation.



4.2 Near-Threshold Operation

At near-threshold, variability compromises the FA circuits on some cases making the SUM output the critical path instead of the Carry-out generation, observing the maximum values found. Table 4.3 presents the results of the near-threshold operation 

The energy results to near-threshold operation are presented in Table 4.4. Operating at low voltage reduces the mean energy over 30% for CMOS, TFA and Hybrid FAs and at least 15% of TGA compared to nominal voltage operation. As stated on (DOKANIA; ISLAM, 2015), the ST technique at NT operation reduces the delay and energy deviation for all circuits. However, the deviation of the circuits is considerably higher at NT operation, emphasizing the need of circuit strategies to deal with variability. 

TFA and TGA showed the highest deviations and unacceptable maximum delays,  which is expected due to their pass-transistor logic and inherent signal degradation. The Hybrid adder showed higher deviations, delays and similar energy consumption in comparison to the CMOS Adder. Given that, the CMOS adder remains as a good choice for low power applications.

Results make clear the advantage of the technique when considering energy variability robustness. Fig. 4.2 shows the comparative evaluation of the improvement reached by ST technique at NT operation. Even when there was a worsening on delay robustness, the energy robustness presented improvements. The technique can introduce more delay variability given that variability determines the ST behavior as well, influencing its delays, which stacks with the impact of multiple transistors in a series arrangement.

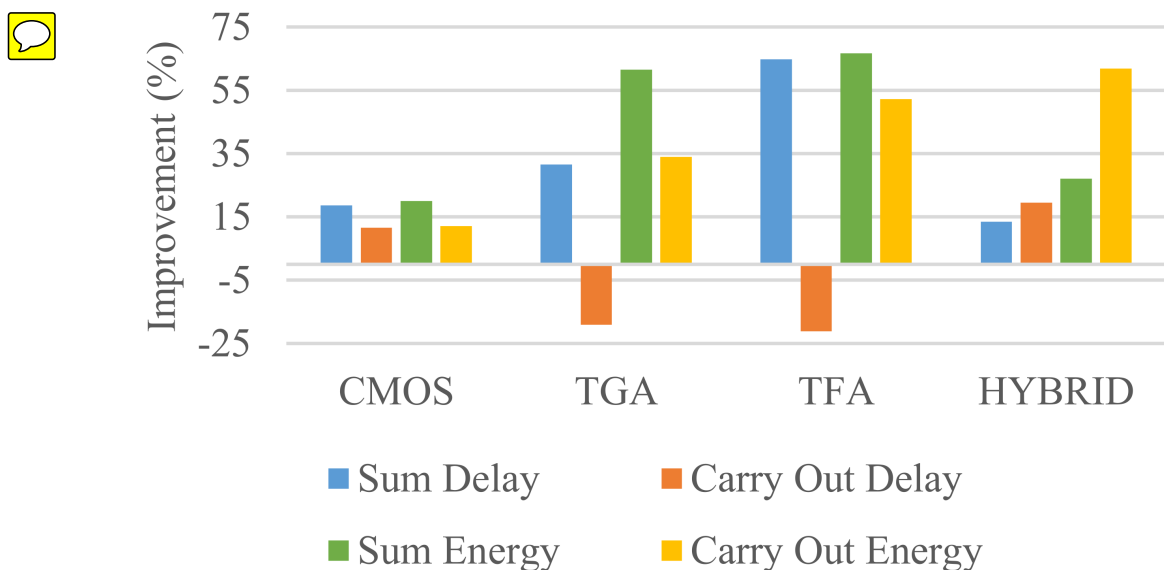
Table 4.3: Delay measures for near-threshold operation.

@NT	Delay									
	SUM					CARRY OUT				
	Max (ps)	μ (ps)	σ (ps)	σ/μ (%)	Δ (%)	Max (ps)	μ (ps)	σ (ps)	σ/μ (%)	Δ (%)
CMOS	873.41	73.22	56.38	77.47	18.70	794.87	128.65	86.67	67.39	11.61
CMOS ST	430.85	95.85	60.57	62.99		539.77	143.77	85.67	59.57	
TGA	7328.30	62.90	92.17	133.30	31.53	6396.90	325.25	138.02	173.54	-19.14
TGA ST	2386.40	127.54	106.22	91.26		6265.10	181.01	373.37	206.76	
TFA	1024.90	67.28	93.48	289.41	64.74	5734.20	151.02	286.55	227.50	
TFA ST	4202.20	84.34	79.51	102.05		6705.80	94.87	233.09	275.63	-21.16
HYBRID	830.64	95.23	77.95	79.00	13.43	695.28	78.00	56.73	73.90	
HYBRID ST	1212.00	120.92	86.26	68.39		2755.30	168.92	100.34	59.51	19.48

Table 4.4: Energy measures for near-threshold operation.

@NT	Energy									
	SUM					CARRY OUT				
	Max (fJ)	μ (fJ)	σ (fJ)	σ/μ (%)	Δ (%)	Max (fJ)	μ (fJ)	σ (fJ)	σ/μ (%)	Δ (%)
CMOS	45.37	6.29	2.00	31.81	20.07	51.91	9.97	2.09	20.97	
CMOS ST	60.64	10.22	2.60	25.43		70.97	15.16	2.80	18.45	12.02
TGA	53.90	6.06	2.01	33.17	61.45	61.28	6.40	1.85	28.90	34.04
TGA ST	34.33	11.30	1.44	12.79		85.49	11.67	2.22	19.06	
TFA	16.26	2.40	0.65	27.05	66.59	23.03	2.58	0.64	24.66	52.18
TFA ST	18.85	5.45	0.49	9.04		22.21	5.61	0.66	11.79	
HYBRID	56.96	6.02	2.29	38.04	27.06	59.99	9.46	2.00	21.19	
HYBRID ST	81.05	11.65	3.23	27.75		26.22	15.03	1.21	8.07	61.91

Figure 4.2: Robustness improvements for each Full Adder at near-threshold operation.



4.3 Penalties

It is expected that a technique which replaces a 2-transistor sub-circuit to a 4-transistor one should bring an impact over metrics. Given so, the average impact at nominal operation was 30% over the delay and their deviations. For energy, the impact is considerable, being on average over 85% percent higher the energy consumption. For energy standard deviations there was a 40% increase at nominal level and a minor 4% increase at near-threshold level. Energy penalties are plotted at Images 4.3 to 4.6.



Figure 4.3: Energy measures for the Sum output at Nominal operation.

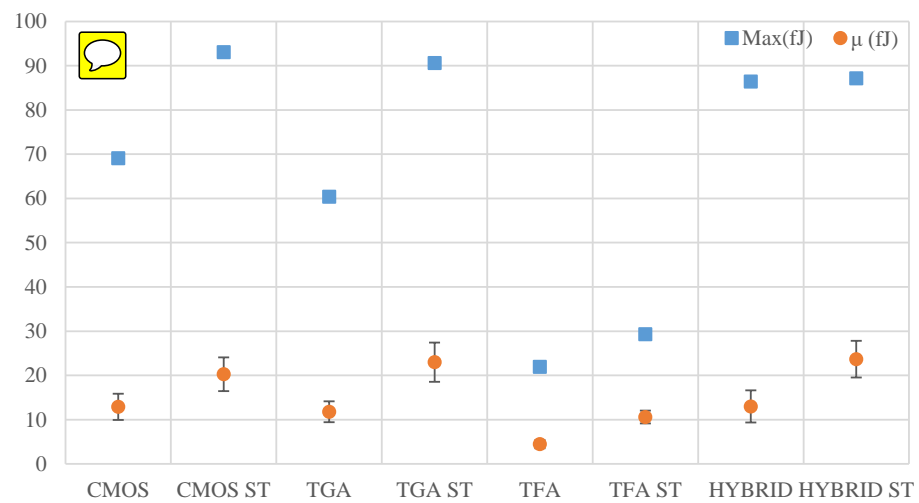
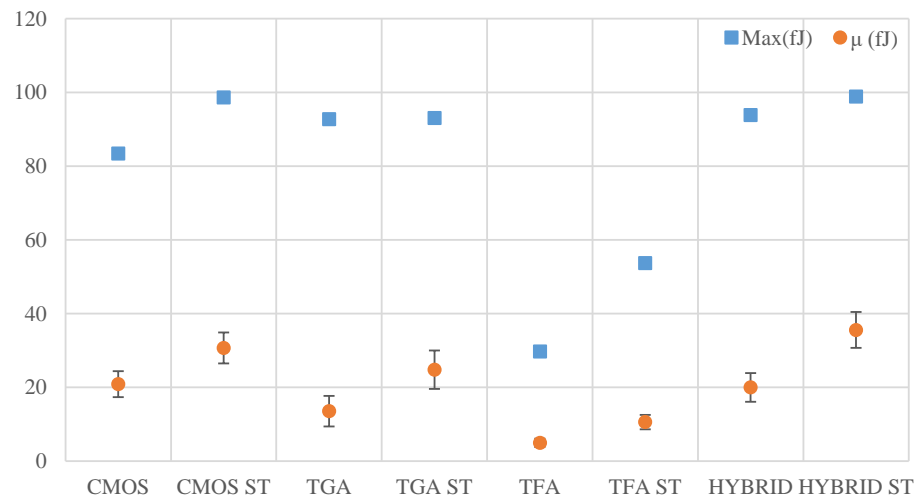


Figure 4.4: Energy measures for the Carry Out output at Nominal operation.



For area penalties there was 150%, 187.5%, 100% and 207% increase for the CMOS, TGA, TFA and Hybrid Full Adders, respectively. Their respective areas, not considering the TAP-Cell area, are shown in Table 4.5. Such high area penalties are



Figure 4.5: Energy measures for the Sum output at Near-Threshold operation.

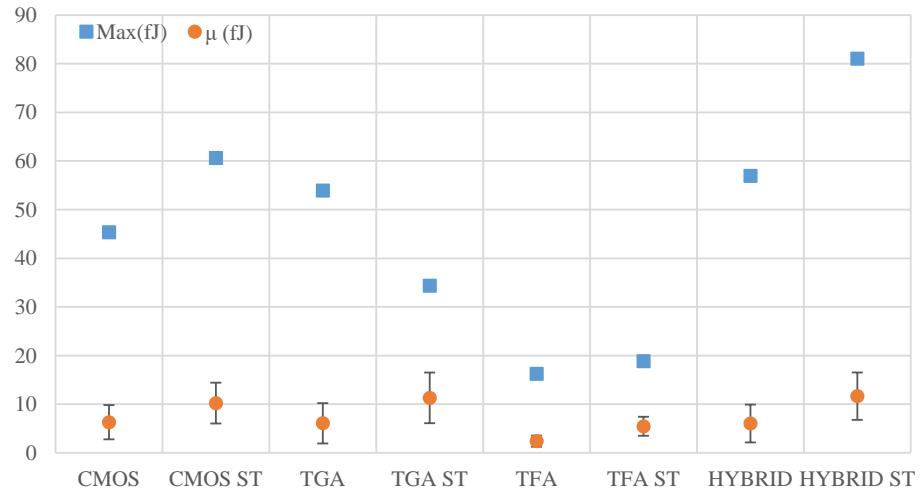
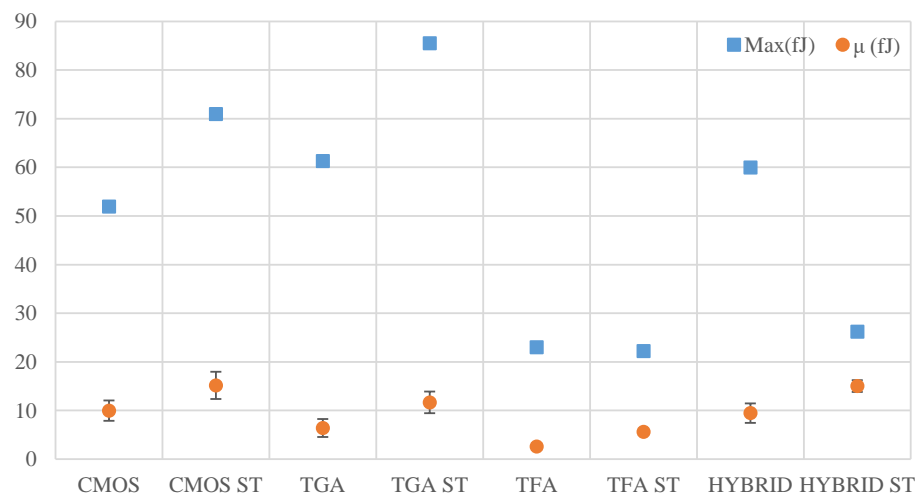


Figure 4.6: Energy measures for the Carry Out output at Near-Threshold operation.

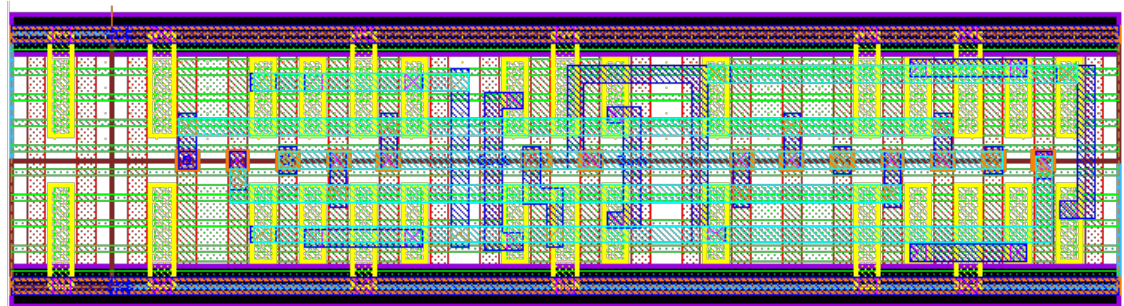


mainly due to technology rules such as the 108nm well-spacing and the necessity to use TAP-Cells to explicitly connect the transistors bulk to specific parts of the circuits or the supply/ground making the ST cell more prominent than expected. The FAs respective layouts are shown in Images 4.7 to 4.10.

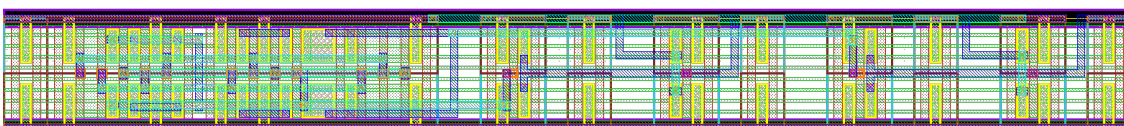
Table 4.5: Full Adders areas and respective technique area impact.

Full Adder	Area (μm^2)	Ratio
CMOS	0.34	2.5
CMOS ST	0.85	
TGA	0.54	2.875
TGA ST	1.56	
TFA	0.47	2
TFA ST	0.95	
HYBRID	0.51	3.07
HYBRID ST	1.56	

Figure 4.7: Original Mirror CMOS (a) and Mirror CMOS with ST technique (b) layouts.

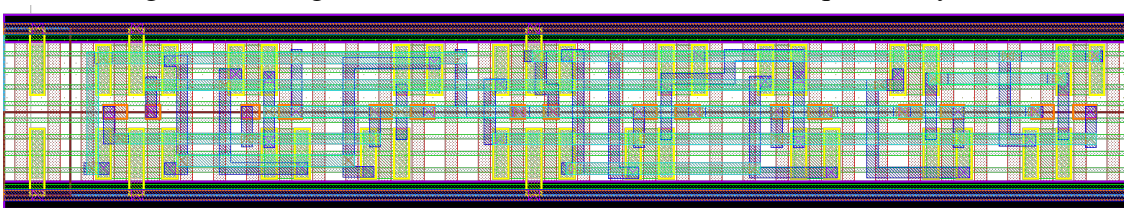


(a)



(b)

Figure 4.8: Original TGA (a) and TGA with ST technique (b) layouts.



(a)



(b)

Figure 4.9: Original TFA (a) and TFA with ST technique (b) layouts.

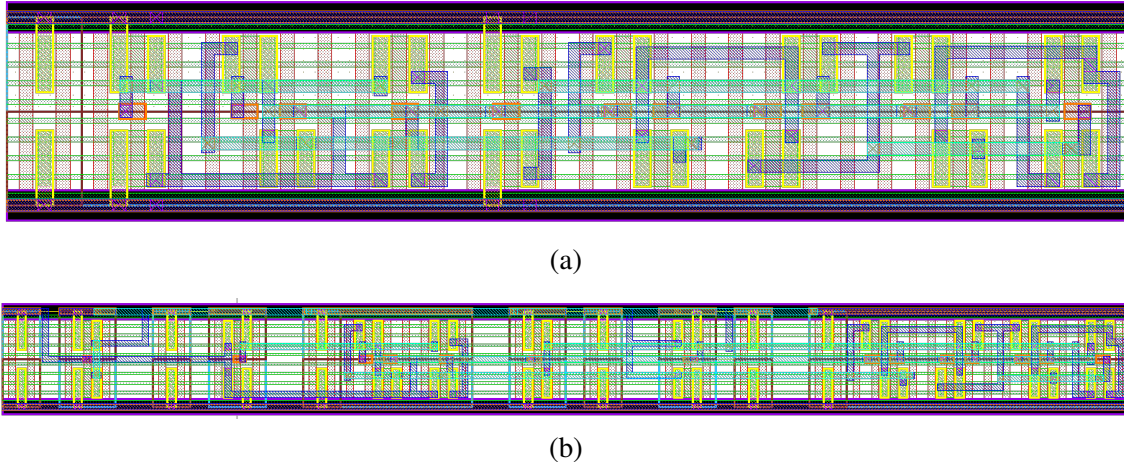
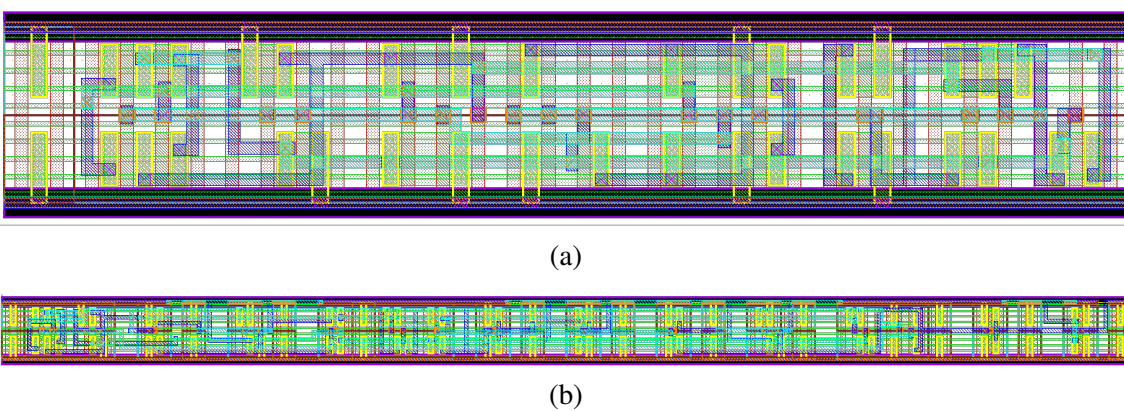


Figure 4.10: Original HYBRID (a) and HYBRID with ST technique (b) layouts.



5 CONCLUSIONS

Variability has been a critical challenge in emerging technology nodes because it can deviate from the correct circuit's behavior and affects the manufacturing yield. All current work in developing and validating techniques have been done at electrical and transistor level. There is a need for novel techniques which to improve variability robustness at the layout level.

Given that, a novel technique was tested. The method consists of replacing internal inverters with Schmitt Trigger inverters to increase the circuit's noise-immunity. The ST technique presents considerable robustness improvements over all full adders. For nominal and near-threshold operation, TFA and Hybrid adders showed the highest accumulated improvements, respectively. As results show, the technique improves, sometimes drastically, the energy variability robustness for each Full Adder considered. For delay robustness, in some cases, there was a worsening in robustness mainly caused by area penalty and the pass-transistor logic.

With the technique penalties in mind, it should only be utilized in applications that can bear the delays, energy consumption and area increase with variability robustness as a priority. These works demonstrate the need for new techniques at layout level to address variability for high performance/low power applications with low area penalties. It is important to note that, according to the state-of-art research, this is the first analysis of this technique made at layout level. For future works, a supply voltage calibration shall be made to find the best cost-benefit supply voltage.



REFERENCES

- ABBAS, Z. et al. Optimal nbti degradation and pvt variation resistant device sizing in a full adder cell. In: **IEEE. Reliability, Infocom Technologies and Optimization (ICRITO)(Trends and Future Directions), 2015 4th International Conference on.** [S.I.], 2015. p. 1–6.
- AGHABABA, H.; AFZALI-KUSHA, A.; FOROUZANDEH, B. Static power optimization of a full-adder under front-end of line systematic variations. In: **IEEE. Design and Test Workshop (IDT), 2009 4th International.** [S.I.], 2009. p. 1–6.
- AHMAD, S. et al. Single-ended schmitt-trigger-based robust low-power sram cell. In: . [S.I.]: IEEE, 2016. v. 24, n. 8, p. 2634–2642.
- AHMADI, M.; ALIZADEH, B.; FOROUZANDEH, B. A hybrid time borrowing technique to improve the performance of digital circuits in the presence of variations. In: . [S.I.]: IEEE, 2017. v. 64, n. 1, p. 100–110.
- ALIOTO, M.; PALUMBO, G. Delay variability due to supply variations in transmission-gate full adders. In: **IEEE. Circuits and Systems, 2007. ISCAS 2007. IEEE International Symposium on.** [S.I.], 2007. p. 3732–3735.
- AMES, S. O. et al. Investigating pvt variability effects on full adders. In: **IEEE. Power and Timing Modeling, Optimization and Simulation (PATMOS), 2016 26th International Workshop on.** [S.I.], 2016. p. 155–161.
- BECKETT, P. A fine-grained reconfigurable logic array based on double gate transistors. In: **IEEE. Field-Programmable Technology, 2002.(FPT). Proceedings. 2002 IEEE International Conference on.** [S.I.], 2002. p. 260–267.
- CLARK, L. T. et al. Asap7: A 7-nm finfet predictive process design kit. In: . [S.I.]: Elsevier, 2016. v. 53, p. 105–115.
- COCKRILL, C. **Understanding Schmitt Triggers - Application Report.** 2011. Available from Internet: <<http://www.ti.com/lit/an/scea046/scea046.pdf>>.
- DEVADAS, M.; KISHORE, K. L. Design topologies for low power cmos full adder. In: **IEEE. Inventive Systems and Control (ICISC), 2017 International Conference on.** [S.I.], 2017. p. 1–4.
- DOKANIA, V.; IMRAN, A.; ISLAM, A. Investigation of robust full adder cell in 16-nm cmos technology node. In: **IEEE. Multimedia, Signal Processing and Communication Technologies (IMPACT), 2013 International Conference on.** [S.I.], 2013. p. 207–211.
- DOKANIA, V.; ISLAM, A. Circuit-level design technique to mitigate impact of process, voltage and temperature variations in complementary metal-oxide semiconductor full adder cells. In: . [S.I.]: IET, 2015. v. 9, n. 3, p. 204–212.
- DOKI, B. L. Cmos schmitt triggers. In: **IET. IEE Proceedings G-Electronic Circuits and Systems.** [S.I.], 1984. v. 131, n. 5, p. 197–202.

- FEDERSPIEL, X. et al. 28nm node bulk vs fdsoi reliability comparison. In: **IEEE. Reliability Physics Symposium (IRPS), 2012 IEEE International**. [S.l.], 2012. p. 3B–1.
- GUDURI, M.; ISLAM, A. Design of hybrid full adder in deep subthreshold region for ultralow power applications. In: **IEEE. Signal Processing and Integrated Networks (SPIN), 2015 2nd International Conference on**. [S.l.], 2015. p. 931–935.
- ISLAM, A. et al. Design and analysis of robust dual threshold cmos full adder circuit in 32nm technology. In: **IEEE. Advances in Recent Technologies in Communication and Computing (ARTCom), 2010 International Conference on**. [S.l.], 2010. p. 418–420.
- ISLAM, A.; AKRAM, M. W.; HASAN, M. Variability immune finfet-based full adder design in subthreshold region. In: **IEEE. Devices and Communications (ICDeCom), 2011 International Conference on**. [S.l.], 2011. p. 1–5.
- ISLAM, A.; HASAN, M. Design and analysis of power and variability aware digital summing circuit. In: . [S.l.: s.n.], 2011. v. 2, n. 2, p. 6–14.
- MEINHARDT, C.; ZIMPECK, A. L.; REIS, R. Impact of gate workfunction fluctuation on finfet standard cells. In: **IEEE. Electronics, Circuits and Systems (ICECS), 2014 21st IEEE International Conference on**. [S.l.], 2014. p. 574–577.
- MOGHADDAM, M.; MOAIYERI, M. H.; ESHGHI, M. Design and evaluation of an efficient schmitt trigger-based hardened latch in cntfet technology. In: . [S.l.]: IEEE, 2017. v. 17, n. 1, p. 267–277.
- NASSIF, S. Process variability at the 65nm node and beyond. In: **IEEE. Custom Integrated Circuits Conference, 2008. CICC 2008. IEEE**. [S.l.], 2008. p. 1–8.
- NAVI, K. et al. A novel low-power full-adder cell for low voltage. In: . [S.l.]: Elsevier, 2009. v. 42, n. 4, p. 457–467.
- RAHIMI, A.; BENINI, L.; GUPTA, R. K. Variability mitigation in nanometer cmos integrated systems: A survey of techniques from circuits to software. In: . [S.l.]: IEEE, 2016. v. 104, n. 7, p. 1410–1448.
- SHAMS, A. M.; BAYOUMI, M. A. A novel high-performance cmos 1-bit full-adder cell. In: . [S.l.]: IEEE, 2000. v. 47, n. 5, p. 478–481.
- SHOARINEJAD, A.; UNG, S.; BADAWY, W. Low-power single-bit full adder cells. In: . [S.l.]: IEEE, 2003. v. 28, n. 1, p. 3–9.
- TAUR, Y.; NING, T. H. **Fundamentals of modern VLSI devices**. [S.l.]: Cambridge university press, 2013.
- TOLEDO, S. P.; ZIMPECK, A. L.; MEINHARDT, C. Impact of schmitt trigger inverters on process variability robustness of 1-bit full adders. In: **IEEE. Conference on Electronics, Circuits and Systems (ICECS)**. [S.l.], 2016.
- WALKER, J. A. et al. Optimizing electronic standard cell libraries for variability tolerance through the nano-cmos grid. In: . [S.l.]: The Royal Society, 2010. v. 368, n. 1925, p. 3967–3981.

WANG, X. et al. Statistical threshold-voltage variability in scaled decananometer bulk hkmg mosfets: A full-scale 3-d simulation scaling study. In: . [S.l.]: IEEE, 2011. v. 58, n. 8, p. 2293–2301.

WESTE, N. H. E.; ESHRAGHIAN, K. **Principles of CMOS VLSI design.** [S.l.]: Addison-Wesley New York, 1985.

ZHANG, C.; SRIVASTAVA, A.; AJMERA, P. K. Low voltage cmos schmitt trigger circuits. In: . [S.l.]: IET, 2003. v. 39, n. 24, p. 1696–1698.

ZIMPECK, A. L. et al. Finfet cells with different transistor sizing techniques against pvt variations. In: **IEEE. Circuits and Systems (ISCAS), 2016 IEEE International Symposium on.** [S.l.], 2016. p. 45–48.

